J. theor. Biol. (1998) **191,** 299–308

Intercellular Spiral Waves of Calcium

MATTHEW WILKINS*§ AND JAMES SNEYD†‡

**Department of Mathematics and Statistics, University of Canterbury, Christchurch, New Zealand and †Department of Mathematics, University of Michigan, 2072 East Hall, 525 East University Avenue, Ann Arbor, MI, 48109-1109, U.S.A.*

(*Received on* 14 *July* 1997, *Accepted in revised form on* 5 *November* 1997)

Intercellular calcium waves have been observed in a large number of cell types, and are known to result from a variety of stimuli, including mechanical or hormonal stimulation. Recently, spiral intercellular waves of calcium have been observed in slices of hippocampal tissue. We use an existing model to study the properties of spiral intercellular calcium waves. Although intercellular spiral waves are well known in the context of cardiac muscle, due to the small value of the calcium diffusion coefficient intercellular calcium waves have fundamentally different properties. We show that homogenisation techniques give a good estimate for the plane wave speed, but do not describe spiral behaviour well. Using an expression for the effective diffusion coefficient we estimate the intercellular calcium permeability in liver. For the bistable equation, we derive an analytic estimate for the value of the intercellular permeability at which wave propagation fails. In the calcium wave model, we show numerically that the spiral period is first a decreasing, then an increasing, function of the intercellular permeability. We hypothesise that this is because the curvature of the spiral core is unimportant at low permeability, the period being approximately set instead by the speed of a plane wave along a line of coupled cells in one dimension.

1. Introduction

In the past few years, a great deal of evidence has accumulated that intracellular and intercellular calcium (Ca^{2+}) signalling is one of the crucial methods of cellular coordination and control. Oscillations in the concentration of free intracellular Ca^{2+} are thought to play an important role in many cellular processes, such as secretion, reproduction and movement, and in many cells these oscillations are organised into periodic intracellular waves (Berridge, 1993; Rooney & Thomas, 1993).

Calcium waves have also been often observed travelling between cells, presumably coordinating cellular responses over much larger regions. For instance, mechanically stimulated Ca^{2+} waves have been observed propagating through ciliated tracheal epithelial cells (Sanderson *et al*., 1990, Boitano *et al*., 1992), rat brain glial cells (Charles *et al*., 1991, 1992, 1993), and many other cell types (Sanderson *et al*., 1994). Furthermore, intercellular Ca^{2+} waves have been observed passing from glial cells to neurons, and vice versa (Charles, 1994; Nedergaard, 1994; Parpura *et al*., 1994). Particularly interesting are recent discoveries that spontaneous intercellular Ca^{2+} waves exist in tissue slice preparations from the hippocampus (Dani *et al*., 1992), and in the intact liver (Robb-Gaspers & Thomas, 1995) and thus are not an artifact of the cell culture or the mechanical stimulus. When a hippocampal slice is stimulated by bath application of N-methyl-D-aspartate (NMDA), intercellular glial Ca^{2+} waves are immediately observed. Since glial cells do not respond directly to NMDA, it is likely that the glial responses result from the release of glutamate by neurons which have been stimulated by the NMDA. Hippocampal intercellular Ca^{2+}

‡Author to whom correspondence should be addressed.
E-mail: jsneyd@math.lsa.umich.edu
§Present address: Courant Institute, New York University, New York, U.S.A.

0022–5193/98/070299 + 10 $25.00/0/jt970585

waves are highly structured, with forms similar to the spatio-temporal organisation of wave activity seen in *Xenopus* oocytes. In particular, intercellular Ca^{2+} waves in hippocampal slices have recently been observed to form spontaneous spiral waves (Harris–White *et al*., 1998. Similar intercellular Ca^{2+} waves, travelling at similar speeds (7–45 $\mu m\ s^{-1}$), have been observed in the intact liver (Robb-Gaspers & Thomas, 1995). Perfusion of a rat liver with vasopressin causes intracellular Ca^{2+} oscillations that are similar to those observed in isolated hepatocytes. Most interesting is the observation that the intracellular oscillations are coordinated over large spatial areas, and thus form coherent intercellular waves that propagate along the hepatic plates. A pacemaker region of the liver acts as an initiating center, and the intercellular waves spread from this region. Each intercellular wave consists of a sequence of intracellular waves, and the delay in intercellular transmission decreases with increasing agonist concentration.

It is widely believed that intercellular Ca^{2+} waves are a mechanism by which a group of cells can communicate with one another, and coordinate a multicellular response to a local event. An understanding of the mechanisms underlying intercellular Ca^{2+} waves is of importance, not only for a general understanding of intercellular communication, but also for the understanding of a wide range of specific processes such as mucociliary clearance, wound healing, mechanical transduction, cell growth, and information processing. For example, in ciliated tracheal epithelial cells the rate of ciliary motion increases as the intracellular Ca^{2+} concentration increases. Thus, an intercellular Ca^{2+} wave would serve to coordinate the ciliary beating of a number of adjacent cells, resulting in more efficient mucus clearance. Intercellular Ca^{2+} waves are also implicated in the wound healing response. If a monolayer of epithelial cells is mechanically damaged, the resultant intercellular Ca^{2+} wave sets up intercellular Ca^{2+} gradients which influence the initiation and direction of cell migration (Sanderson *et al*., 1994). Not well understood, but potentially of extreme significance, are recent findings that intercellular Ca^{2+} waves in glial cells can be communicated to neurons, and thus glial cells could play an active role in information processing (Charles, 1994; Nedergaard 1994; Parpura *et al*., 1994; Hassinger *et al*., 1995). Intercellular Ca^{2+} waves in glia have also been linked to spreading depression in the brain, in which waves of depolarisation spread at a similar speed to intercellular Ca^{2+} waves in glia (Leibowitz, 1992).

2. The Mechanism of Intercellular Waves

Intracellular calcium signalling has been intensively studied in many cell types, and there is general agreement on the initial steps of the calcium response (Berridge, 1993). When an agonist binds to its receptor, it initiates a series of reactions that results in the production of a chemical called inositol 1,4,5-trisphosphate (IP_3). IP_3 diffuses through the cell cytoplasm and binds to IP_3 receptors located on the endoplasmic reticulum (ER) and the nuclear membrane. IP_3 receptors are also Ca^{2+} channels, and when IP_3 binds, they open, releasing large amounts of Ca^{2+} from the ER. Note that, at steady state, the concentration of Ca^{2+} in the ER is high, and thus there is a steep concentration gradient of Ca^{2+} between the ER and the cytoplasm. Released Ca^{2+} then activates the IP_3 receptors, leading to the release of further Ca^{2+}, in an autocatalytic process called Ca^{2+}-induced Ca^{2+} release (CICR). Release of Ca^{2+} through the IP_3 receptor is terminated when high cytoplasmic Ca^{2+} concentrations inactivate the receptor. Thus, Ca^{2+} has both a positive and a negative feedback effect on the IP_3 receptor. Ca^{2+} pumps actively remove Ca^{2+} from the cytoplasm, pumping it back into the ER or out of the cell, until the cell returns to steady state. The cytoplasm is an excitable medium (with respect to Ca^{2+} release) in much the same way that the nerve axon is an excitable medium with respect to electrical potential.

Such a mechanism has been used by a number of groups to explain propagating waves of Ca^{2+} inside single cells, and their organisation into intracellular spiral waves (Lechleiter & Clapham, 1992; Atri *et al*., 1993; Dupont & Goldbeter, 1994; Sneyd *et al*., 1995b). Other groups have hypothesised that the coupling of excitable cells by gap junctions could also lead to the propagation of intercellular Ca^{2+} waves of the types observed experimentally. For instance, since it is known that vasopressin causes the production of IP_3, it has been hypothesised (Robb-Gaspers & Thomas, 1995) that intercellular waves in liver are the result of the coupling of excitable intracellular Ca^{2+} dynamics by an intercellular messenger. Further, the direction of the intercellular waves is not altered by the direction of the perfusion, suggesting that the intercellular messenger is communicated through gap junctions. Since glial cells in hippocampal explants are extensively coupled by gap junctions, a similar hypothesis has been proposed to explain intercellular Ca^{2+} waves in hippocampal explants (Dani *et al*., 1992).

It is important to note that the intercellular waves described above are fundamentally different from the

mechanically-stimulated waves described and modelled by Sanderson and his colleagues (Sanderson *et al*., 1994; Sneyd *et al*., 1994, 1995a). Their hypothesis is that mechanically-stimulated intercellular waves result from the passive diffusion of IP_3 from the stimulated cell and are not actively propagated. Clearly, such a mechanism could not possibly result in a spiral wave, and is therefore not applicable to the observed waves in hippocampal slice explants.

Our goal is to study the properties of intercellular Ca^{2+} waves in a fairly general framework. Our results are not tied to the details of any specific model (although we perform most of our simulations using a particular model), but are applicable to any system in which intercellular waves are propagated by coupled excitable systems. Similar systems have been studied in detail in the context of cardiac electrophysiology. However, we shall show that, because the Ca^{2+} diffusion coefficient is so small, intercellular Ca^{2+} waves have some unique properties.

3. The Model

Our model and numerical computations are based on the model of Atri *et al*. (1993) that was originally designed to model intracellular spiral Ca^{2+} waves in *Xenopus* oocytes. Here, only the bare essentials of the model will be presented.

The model equations are

$$\frac{\partial c}{\partial t} = D_c\left(\frac{\partial^2 c}{\partial x^2} + \frac{\partial^2 c}{\partial y^2}\right) + J_{\text{flux}} - J_{\text{pump}}, \tag{1}$$

$$J_{\text{pump}} = \frac{\gamma c}{k_\gamma + c}, \tag{2}$$

$$J_{\text{flux}} = k_f \mu(p)\left(b + \frac{(1-b)c}{k_1 + c}\right)h, \tag{3}$$

$$\tau_h \frac{\mathrm{d}h}{\mathrm{d}t} = \frac{k_2^2}{k_2^2 + c^2} - h, \tag{4}$$

$$\mu(p) = \frac{p}{k_\mu + p}, \tag{5}$$

where $c = [Ca^{2+}]$ and $p = [IP_3]$.

J_{pump} describes the amount of Ca^{2+} being pumped out of the cytoplasm back into the ER or out through the plasma membrane. J_{flux} models the flux of $[Ca^{2+}]$ through the IP_3 receptor, and depends on the fact that Ca^{2+} activates the IP_3 receptor quickly, but inactivates it on a slower time-scale. The binding sites for IP_3 and Ca^{2+} are assumed to be independent.

$\mu(p)$ is the fraction of IP_3 receptors that have bound IP_3, and is an increasing function of p. The term $b + (1-b)c/(k_1 + c)$ controls the activation of the IP_3 receptor by Ca^{2+}. It is assumed that Ca^{2+} instantaneously activates the IP_3 receptor. The variable h denotes the fraction of IP_3 receptors that have not been inactivated by Ca^{2+}. At steady state $h = k_2^2/(k_2^2 + c^2)$, a decreasing function of $[Ca^{2+}]$. Inactivation by Ca^{2+} is assumed to act on a slower time-scale, with time constant τ_h. The constant k_f denotes the Ca^{2+} flux when all IP_3 receptors are open and activated.

Equation (1) only applies within each cell, not across the entire culture. At the boundaries between cells it is assumed that the flux across the cell membrane is proportional to the concentration difference across the membrane. For instance, consider a membrane situated at $x = 0$ in one spatial dimension. Then,

$$D_c\frac{\partial c(0^-,t)}{\partial x} = D_c\frac{\partial c(0^+,t)}{\partial x} = F_c[c(0^+,t) - c(0^-,t)], \tag{6}$$

where superscripts $-$ and $+$ denote limits from the left and right respectively. In our simulations, all cell boundaries are oriented along one of the coordinate axes, and the equations are discretised with a regular grid aligned with the coordinate axes. All cell boundaries are assumed to lie between grid points. Thus, difficulties caused by the orientation of the boundary are avoided.

The parameter values were obtained by experimental measurements in a variety of cell types (Atri *et al*., 1993). Although there is no reason to believe that these are the correct values for glial cells, no better measurements are presently available. In any case, as we pointed out above, our results do not depend qualitatively on the details of the model. In Table 1 we give the parameters and their numerical values.

4. Oscillations and Intracellular Waves in the Model

First we note that intercellular spiral waves in hippocampal slices are produced experimentally by a bath application of NMDA, which, presumably, raises the concentration of IP_3 approximately uniformly over the entire tissue slice. Thus, we may assume that p is fixed, and treat it like a bifurcation parameter. Equivalently, we may use μ as the bifurcation parameter. Different fixed values of μ will give different model behaviour. In the absence of diffusion, as the value of μ increases, stable limit cycles appear via a homoclinic bifurcation (Fig. 1).

When μ is less than, but close to, the value at which the homoclinic bifurcation occurs, the model with diffusion exhibits travelling waves (Fig. 2). To give the desired value of $\mu(p)$, an initial $[IP_3]$ of 0.672 μM is

TABLE 1
The parameter values of the model [taken from Atri et al. (1993)]

Parameter	Explanation	Value
b	Fraction of activated IP_3 receptors when $[Ca^{2+}] = 0$	0.111
k_1	K_m for activation of IP_3 receptors by Ca^{2+}	0.7 μM
k_2	K_m for inactivation of IP_3 receptors by Ca^{2+}	0.7 μM
D_c	Diffusion coefficient of Ca^{2+}	20 $(\mu m)^2\ s^{-1}$
γ	Maximum rate of pumping of ER Ca^{2+} pumps	2 μM/s
k_f	Ca^{2+} flux when all IP_3 receptors are open and activated	16.2 μM/s
k_γ	K_m of endoplasmic reticulum Ca^{2+} pumps	0.1 μM
k_μ	K_m for binding of IP_3 to its receptor	0.7 μM
τ_h	Time constant for inactivation of IP_3 receptors	2 s

placed over the whole domain. The $[Ca^{2+}]$ is initially at steady state, which, for the numerical values in Table 1, is 0.13 μM. To start the travelling wave, 1 μM of Ca^{2+} is added in the first 0.9 μm of the domain on the left-hand side. Travelling waves were produced when the background $[IP_3]$ is approximately between 0.66 μM and 0.673 μM. This narrow range of values for $[IP_3]$ is an unattractive feature of the model, but has no qualitative effect on the results presented here. Other models are more robust with respect to wave generation.

One crucial fact to note about the travelling waves is that the width of the wave front (10 μm or so) is small compared with the length of a typical cell (30 μm). Thus, an entire wave front is contained within a single cell, and indeed the entire wave, front and back, is contained within only two or three cells.

According to the model, the cell cytoplasm is an excitable system, with behaviour similar to that of the FitzHugh–Nagumo model, a generic excitable system.

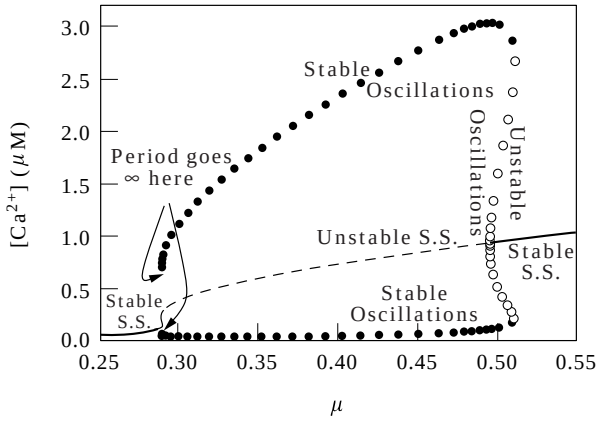

FIG. 1. $[Ca^{2+}]$ versus the bifurcation parameter μ. The line made up of circles shows the maximum and minimum of the $[Ca^{2+}]$ oscillations (filled circles are stable and hollow are unstable). Oscillations occur for μ above about 0.29. Waves occur for μ less than, but close to, 0.29.

Once the Ca^{2+} concentration gets above a threshold value, the autocatalytic process of CICR takes over, and leads to the release of a large amount of Ca^{2+}. Eventually, the high Ca^{2+} concentration shuts off the Ca^{2+} flux through the IP_3 receptor, and the Ca^{2+} concentration returns to steady state. However, although the behaviour of the model is similar to that of the FitzHugh–Nagumo model, it is interesting to note that the structure of the model equations is rather different, as the nullclines do not have the generic shape. This is not an issue we shall explore further here, but just note in passing.

5. Intercellular Plane Waves

Next we consider the propagation of an intercellular plane wave. We solve the model equations,

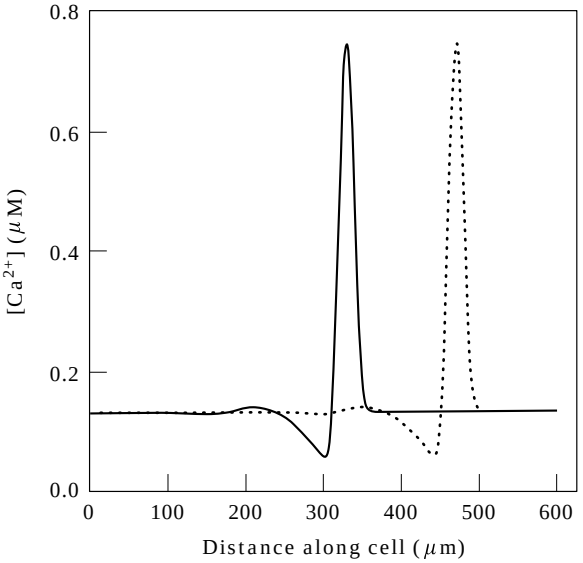

FIG. 2. The wave (in a single large cell) shown at two different times. The wave is travelling at about 7 μm S^{-1}. Key: —— time = 50 s; – – – time = 70 s.

together with the internal boundary conditions (6) on a grid of 20 by 20 cells, each of which has a side length of 30 μm. As before, the domain is primed with IP_3, so $[IP_3]$ is constant over the whole domain. Ca^{2+} is added in on the left-hand side of the domain, and this initiates a wave. However, this time there are cell membranes for the Ca^{2+} wave to get through. Thus, the wave travels across a cell, reaches the membrane at the far end, and then pauses until enough Ca^{2+} has leaked through to initiate a wave in the neighbouring cell. As F_c decreases, it takes longer for a wave in one cell to initiate a wave in the neighbouring cell, and so the intercellular wave speed decreases (Fig. 3). When F_c is below 0.3 μm s^{-1} the wave ceases to propagate at all.

We note that, technically, an intercellular plane wave is not a travelling wave, as it is not translation invariant in space and time. However, although this makes it difficult to construct the wave solutions analytically, it is still possible to obtain estimates for when the wave fails to propagate.

It is interesting to investigate why wave propagation fails when F_c is below a certain critical value. When the wave reaches a membrane the front of the wave stops while Ca^{2+} slowly leaks through the membrane. The $[Ca^{2+}]$ on the other side of the membrane must reach the threshold value before the wave will start to propagate in the next cell. There could be two reasons why the $[Ca^{2+}]$ doesn't reach the threshold. Firstly, the Ca^{2+} may be being pumped away faster than it is leaking through, so the $[Ca^{2+}]$ will never build up sufficiently. Alternatively, the back of the wave could reach the membrane before the $[Ca^{2+}]$ on the other side of the membrane exceeds the threshold.

5.1. PROPAGATION FAILURE IN THE BISTABLE EQUATION

Since the model of Ca^{2+} wave propagation is an excitable system, it is reasonable to expect that some insight into the model's behaviour may be gained by the study of simpler models of excitable systems. Thus, to gain an analytic understanding of propagation failure, we study a simpler model, the generalised bistable equation,

$$\frac{\partial c}{\partial t} = D_c \frac{\partial^2 c}{\partial x^2} + f(c), \tag{7}$$

where $f(c)$ has a generic cubic shape, with roots at $c = 0$, α and 1. It is well known that the generalised bistable equation has a travelling wave solution when $0 < \alpha < 1/2$, and so we restrict ourselves to this case. There has been a considerable amount of work done on the effects of blocks, or gap junctions, on reaction-diffusion equations and wave propagation (Pauwelussen, 1981, 1982; Othmer, 1983; Keener, 1991; Sneyd & Sherratt, 1997). The argument used here is based on the methods presented in Keener (1991).

Since an entire wave front is contained within a single cell, it is sufficient to suppose we have two semi-infinite cells, one extending from $x = -\infty$ to $x = 0$ and the other extending from $x = 0$ to $x = \infty$. The discontinuity in the solution at the cell boundary is given by (6). We look for a standing solution to the bistable equation, under the assumption that a standing solution will preclude the existence of a propagating wave (Fife, 1979; Keener, 1987, 1991; Pauwelussen, 1981, 1982). Although the non-existence of a standing solution does not prove the existence of a propagating wave solution, numerical solutions indicate that, at least for the case considered here, if a standing solution does not exist, a wave solution usually does.

The standing solution must satisfy $c \to 1$ as $x \to -\infty$, and $c \to 0$ as $x \to \infty$. At steady state

$$D_c c'' = -f(c), \tag{8}$$

and so

$$\frac{1}{2}\frac{\mathrm{d}}{\mathrm{d}x}(c')^2 = \frac{\mathrm{d}}{\mathrm{d}x}G(c), \tag{9}$$

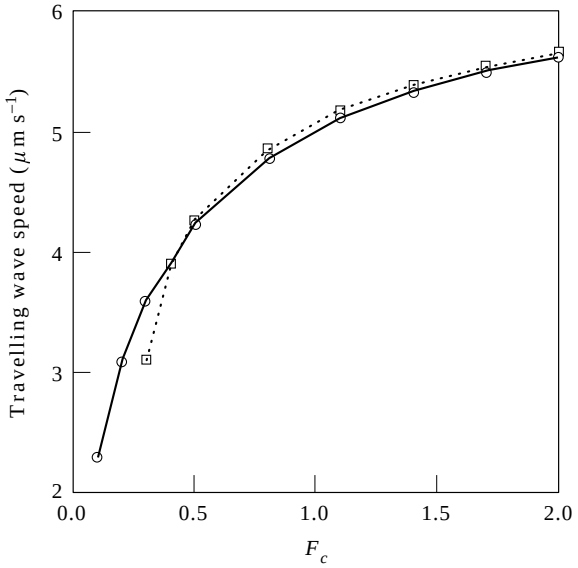

FIG. 3. The wave speed versus F_c for the normal simulations (with cell membranes) and the homogenised equations. As F_c decreases the plane wave speed decreases, but below $F_c = 0.3$ μm s^{-1} the cell boundaries prevent wave propagation. The speed asymptotically increases to about 6.5 μm s^{-1} with increasing F_c. Key: ○, homogenisation; □, normal.

where

$$G(c) = -\frac{1}{D_c}\int_0^c f(v)\mathrm{d}v. \tag{10}$$

It follows that

$$\frac{1}{2}(c')^2 = \begin{cases} G(c) - G(1) & x\in(-\infty,\ 0], \\ G(c), & x\in[0,\ \infty), \end{cases} \tag{11}$$

where we have used the boundary conditions at $\pm\infty$. If we now let c^- denote $c(0^-)$ and similarly for c^+, we get the boundary conditions at $x = 0$,

$$\sqrt{2[G(c^-) - G(1)]} = \frac{F_c}{D_c}(c^- - c^+) = \sqrt{2G(c^+)}. \tag{12}$$

This can now be solved for c^- and c^+. Then, requiring $c^+ < \alpha$ (which is necessary in order for the solution to be valid), we get a relationship between F_c and α that guarantees the existence of a standing solution.

As a particular realisation of this, we choose $f(c) = -c + H(c - \alpha)$ to give the piecewise linear

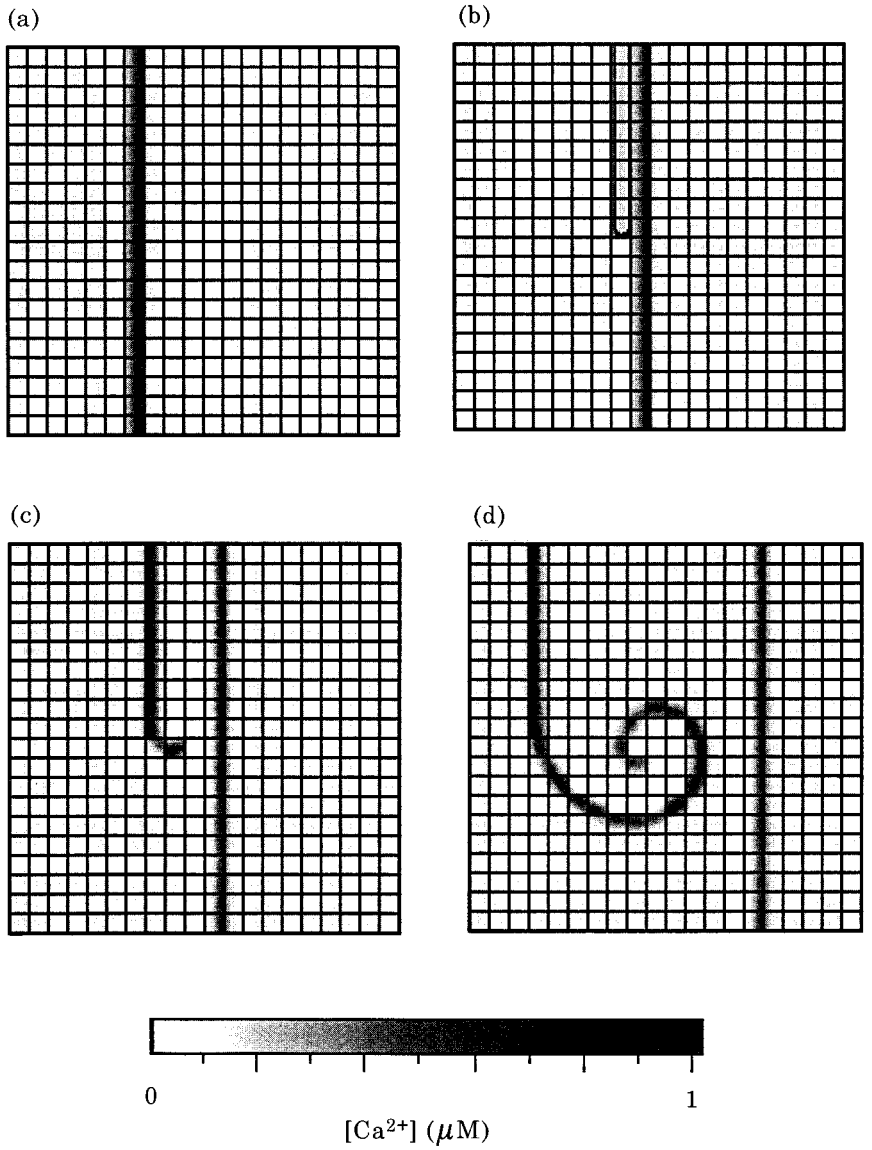

FIG. 4. How an intercellular spiral is created numerically. The cells are 30 μm across. (a) At time = 40 s the initial wave has moved across approximately half the domain. (b) At time = 57.2 s, a bolus of Ca^{2+} (1 μM) is added. (c) At times 65 s the tip of the bolus has curled around and (d) at time 88 s it has developed into a spiral wave. In this simulation $F_c = 1.1$ μm s^{-1}.

bistable equation. In this case, a propagating wave exists only when

$$\frac{F_c}{2F_c + \sqrt{D_c} > \alpha}. \tag{13}$$

When $\alpha = 0.1$ and $D_c = 20$, *a propagating wave exists only when* $F_c > 0.56$. (Of course, this numerical estimate does not necessarily apply to more complex models.)

The analysis above does not take into account the existence of a wave back, which can lead to propagation failure even when F_c is greater than the critical value. For, when F_c is close to the critical value, the wave will take a long time to cross the membrane; this will lead to propagation failure if the wave back catches up to the membrane before the front has progressed through. Thus, the analysis above just gives a lower bound for the critical value of F_c.

6. The Effective Diffusion Coefficient

One common technique used in the study of intercellular waves in cardiac tissue is homogenisation, in which the details of the cell boundaries are replaced by an averaged description (Hunter *et al*., 1975; Keener, 1991; Neu & Krassowska, 1993). Homogenisation smooths out local variations to give an effective diffusion coefficient that ignores variations on the microscopic scale.

Given a line of N cells, each of length L, the effective diffusion coefficient is defined by assuming that an analog of Ohm's law holds. Thus, if $c(0,t) = C_0$ and $c(NL,t) = C_1$, the effective diffusion coefficient, D_e, is defined by

$$J = \frac{D_e}{NL}(C_0 - C_1), \tag{14}$$

where J is the steady state flux. It is a standard result (see, for example, Weidmann, 1966; Hunter *et al*., 1975) that, when L is small with respect to the diffusion space constant,

$$\frac{1}{D_e} = \frac{1}{D_e} + \frac{1}{LF_c}. \tag{15}$$

The assumption that the length of each cell is small compared with the diffusion space constant is an accurate one for wave propagation in cardiac tissue, the context in which this theory is often used. Thus, in typical cardiac tissue, the wave front extends over many cells, the effects of the cell boundaries being merely to add small perturbations to the overall wave shape. The opposite is true however for intercellular Ca^{2+} waves. The diffusion coefficient of Ca^{2+} is only about 20 $\mu m^2\ s^{-1}$, while each cell is about 30 μm long. Thus, the wave front is completely contained within a single cell, and the wave progresses in an intermittent fashion, stopping at the cell boundaries, and travelling quickly across each cell. There is thus no a priori reason to expect that the wave can be modelled by the use of an effective diffusion coefficient.

Nevertheless, numerical computations show that the plane intercellular wave speed is closely approximated by that predicted by the effective diffusion coefficient, as is shown in Fig. 3. At low values of F_c the homogenised theory cannot of course explain propagation failure, but at higher values of F_c the agreement is excellent. However, the homogenised equations do not provide a good description of the intercellular spiral wave.

6.1. ESTIMATING THE INTERCELLULAR PERMEABILITY

Interestingly, the above result gives us a simple way of measuring F_c, the intercellular permeability. Since the wave speed is proportional to the square root of the diffusion coefficient, it follows that $s_p/s_i = \sqrt{D_c}/\sqrt{D_e}$, where s_p is the plane wave speed, and s_i is the intercellular wave speed. Thus, using (15), it follows that

$$F_c = \frac{D_c}{L\left[\left(\frac{s_p}{s_i}\right)^2 - 1\right]}. \tag{16}$$

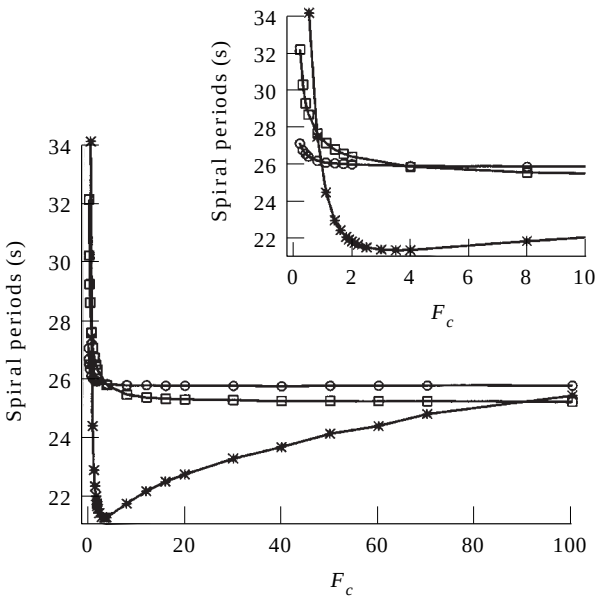

FIG. 5. Period of the intercellular spiral versus F_c for cells of width 30 μm and 1 μm and for the homogenised equations. key: ○, homogenised equations; □, small cells; ∗, normal sized cells.

it is more useful to write this in a different form. If the intercellular wave takes τ seconds to travel between cells, then

$$s_i = \frac{Ls_p}{L + \tau s_p}, \tag{17}$$

where L is the length of an individual cell. Thus,

$$F_c = \frac{D_c}{2\tau s_p + (\tau s_p)^2/L}. \tag{18}$$

From the data of Robb–Gaspers & Thomas (1995) we estimate $L = 25\ \mu\text{m}$, $\tau = 2.5\ \text{s}$, and $s_p = 21\ \mu\text{m s}^{-1}$, which gives $F_c \approx 0.1\ \mu\text{m s}^{-1}$.

7. Intercellular Spiral Waves

It is a relatively simple matter to generate an intercellular spiral, as long as F_c is large enough. Firstly, a wave is set up to propagate across the domain of cells. When it is approximately in the centre, a bolus (in the shape of a line) of Ca^{2+} is placed directly behind the refractory region of the wave. Because of the refractory period of the medium, the bolus cannot spread in the direction of the wave, and thus goes the other way. As it moves, the ends of the bolus start to curl round on themselves thus creating a spiral (Fig. 4). Even though a wave will

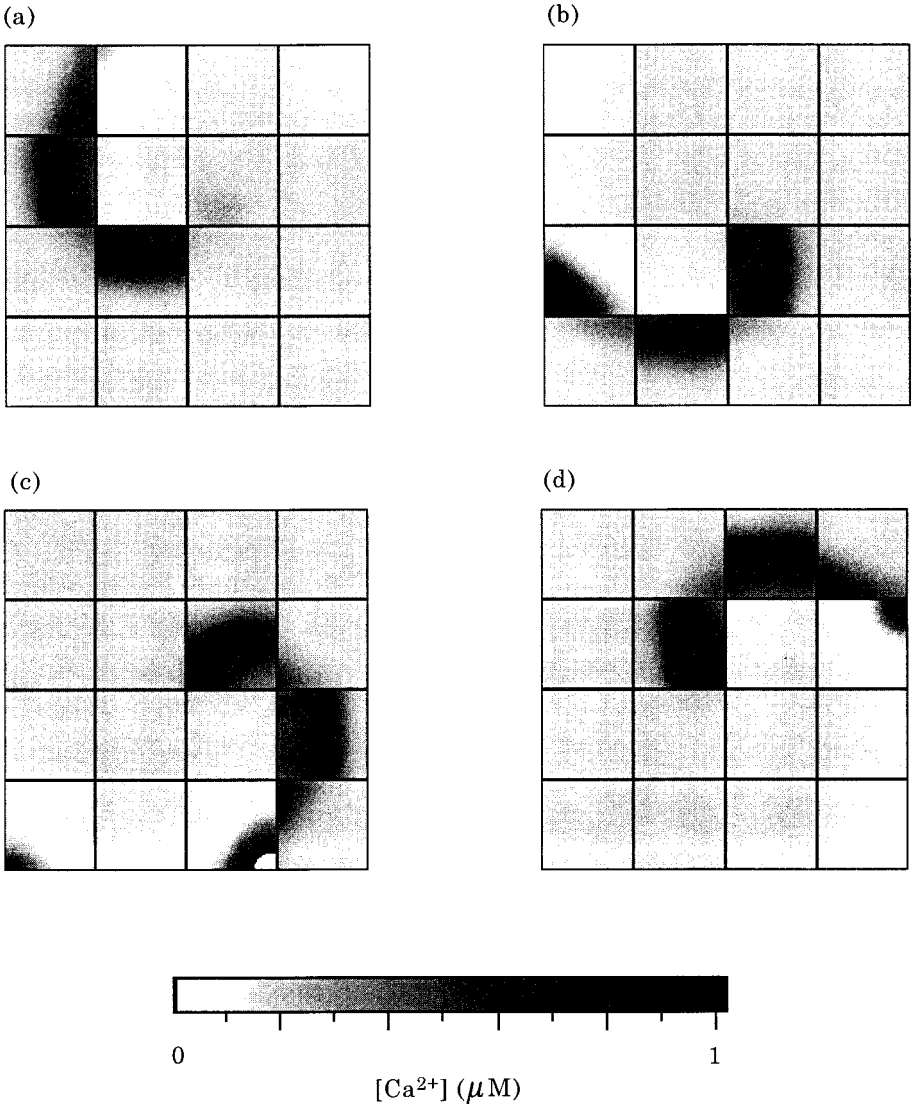

FIG. 6. The core of the intercellular spiral wave when $F_c = 0.5\ \mu\text{m s}^{-1}$. Panels (a–d) are in order of increasing time.

propagate for F_c as low as 0.3 μm s^{-1}, a spiral cannot be formed for such low values of F_c. For $F_c = 0.5$ μm s^{-1} or above the spirals are stable. At $F_c = 0.4$ μm s^{-1} a spiral can be formed, but it is not stable, and breaks up after a few minutes. At $F_c = 0.3$ μm s^{-1} a spiral cannot even be formed. It is interesting to note that the value of F_c estimated from experiments in the intact liver is close to the value needed to propagate an intercellular wave in the model. This confirms that the observed intercellular waves may indeed be the result of the intercellular coupling of excitable cells, as originally proposed.

In Fig. 5 we plot the spiral period versus F_c for three cases: the homogenised equations (using the effective diffusion coefficient), normal sized cells (side length of 30 μm) and very small cells (side length of 1 μm). Firstly, notice that as $F_c \to \infty$ all three lines converge (the period for the small cells is a bit low—this is probably due to discretisation error as the small cells create some numerical difficulties). This convergence is as expected. As $F_c \to \infty$, cell membranes will have no effect on wave propagation. Secondly, the homogenised equations do a good job at predicting the spiral period when the cells are small (and, of course, if F_c is not too small). Again, this is as expected. As the cells get smaller, the assumptions underlying the homogenised equations become more accurate, and thus the theory works better.

However, the homogenised equations do very poorly at predicting the period of the spirals over the larger cells. Not only that, but the spiral period behaves in a fundamentally different manner as a function of F_c. For the other two cases the period is a monotone decreasing function of F_c. This is simply due to the increase in the effective diffusion coefficient, which speeds up the waves, thus decreasing the period. But for the cells of normal size, the period first decreases and then increases as F_c increases. The reasons for this are not completely clear, but an educated guess can be made.

The period of the spiral is governed by the speed at which the core rotates. F_c affects the core in two different ways. With decreasing F_c, any intercellular wave, and thus the core, travels slower because of the increased resistance. However, as F_c decreases the core also loses its curvature, and consists rather of a combination of straight wave portions, interrupted by the cell boundaries. As can be seen from Fig. 6, for $F_c = 0.5$ μm s^{-1} the core is essentially made up of straight wave fronts propagating around a two by two square of cells. Thus, the core of the spiral does not have a high curvature, as do the spiral cores in a homogeneous medium, and so curvature effects do not slow down the spiral core, as is the case in a homogeneous excitable medium (Keener, 1986; Zykov, 1980; Tyson & Keener, 1988). On the contrary, as the spiral core loses curvature it actually speeds up. In summary, as F_c decreases, there are two competing effects; firstly, the decrease in wave speed caused by the decrease in the effective diffusion coefficient, and secondly, an increase in wave speed caused by the loss of curvature. Competition between these two effects causes the non-monotonic behaviour of spiral period as a function of F_c.

We can check this hypothesis in a qualitative fashion by considering the decrease in spiral period at low values of F_c. As F_c increases from 0.5 μm s^{-1} up to 2 μm s^{-1} the plane wave speed increases by a factor of about $5.6/3.1 = 1.32$ and the period goes down by a similar amount of about $34/22 = 1.55$. Hence, it appears that the decrease in spiral period is caused almost entirely by the increased speed of the intercellular plane wave, and curvature is having very little effect. However as F_c increases from about 3 μm s^{-1} the core starts to gain curvature, the increase in the speed of the core is lessened, and so the period increases again.

REFERENCES

Atri, A., Amundson, J., Clapham, D. & Sneyd, J. (1993). A single-pool model for intracellular calcium oscillations and waves in the *Xenopus laevis* oocyte. *Biophys. J.* **65,** 1727–1739.

Berridge, M. J. (1993). Inositol trisphosphate and calcium signalling. *Nature* (*Lond*). **361,** 315–325.

Boitano, S., Dirksen, E. R. & Sanderson, M. J. (1992). Intercellular propagation of calcium waves mediated by inositol trisphosphate. *Science* **258,** 292–294.

Charles, A. C. (1994). Glia-neuron intercellular calcium signaling. *Dev. Neurosci.* **16,** 196–206.

Charles, A. C., Dirksen, E. R., Merrill, J. E. & Sanderson, M. J. (1993). Mechanisms of intercellular calcium signaling in glial cells studied with dantrolene and thapsigargin. *Glia* **7,** 134–145.

Charles, A. C., Merrill, J. E., Dirksen, E. R. & Sanderson, M. J. (1991). Intercellular signaling in glial cells: calcium waves and oscillations in response to mechanical stimulation and glutamate. *Neuron* **6,** 983–992.

Charles, A. C., Naus, C. C. G., Zhu, D., Kidder, G. M., Dirksen, E. R. & Sanderson, M. J. (1992). Intercellular calcium signaling via gap junctions in glioma cells. *J. Cell Biol.* **118,** 195–201.

Dani, J. W., Cherjavsky, A. & Smith, S. J. (1992). Neuronal activity triggers calcium waves in hippocampal astrocyte networks. *Neuron* **8,** 429–440.

Dupont, G. & Goldbeter, A. (1994). Properties of intracellular Ca^{2+} waves generated by a model based on Ca^{2+}-induced Ca^{2+} release. *Biophys. J* **67,** 2191–2204.

Fife, P. (1979). *Mathematical aspects of reacting and diffusing systems*: Berlin: Springer-Verlag.

Harris-White, M. E., Zanotti, S. A., Frautschy, S. A., Charles, A. C. (1998). Spiral intercellular calcium waves in hippocampal slice cultures. *J. Neurophysiol.* **79,** 1045–1052.

Hassinger, T. D., Atkinson, P. B., Strecker, G. J., Whalen, L. R., Dudek, F. E., Kossel, A. H. & Kater, S. B. (1995). Evidence for glutamate-mediated activation of hippocampal neurons by glial calcium waves. *J. Neurobiol.* **28,** 159–170.

Hunter, P. F., McNaughton, P. A. & Noble, D. (1975). Analytical

models of propagation in excitable cells. *Prog. Biophys. Molec. Biol.* **30,** 99–144.

KEENER, J. P. (1986). A geometrical theory for spiral waves in excitable media. *SIAM J. Appl. Math.* **46,** 1039–1056.

KEENER, J. P. (1987). Propagation and its failure in coupled systems of discrete excitable cells. *SIAM J. Appl. Math.* **47,** 556–572.

KEENER, J. P. (1991). The effects of discrete gap junctional coupling on propagation in myocardium. *J. theor. Biol.* **148,** 49–82.

LECHLEITER, J. & CLAPHAM, D. (1992). Molecular mechanisms of intracellular calcium excitability in X. laevis oocytes. *Cell* **69,** 283–294.

LEIBOWITZ, D. H. (1992). The glial spike theory. I. On an active role of neuroglia in spreading depression and migraine. *Proc. R. Soc. Lond. B* **250,** 287–295.

NEDERGAARD, M. (1994). Direct signaling from astrocytes to neurons in cultures of mammalian brain cells. *Science* **263,** 1768–1771.

NEU, J. C. & KRASSOWSKA, W. (1993). Homogenization of syncytial tissues. *Crit. Rev. Biomed. Eng.* **21,** 137–199.

OTHMER, H. G. (1983). A continuum model for coupled cells. *J. Math. Biol.* **17,** 351–369.

PARPURA, V., BASARSKY, T. A., LIU, F., JEFTINIJA, K., JEFTINIJA, S. & HAYDON, P. G. (1994). Glutamate-mediated astrocyte-neuron signaling. *Nature* **369,** 744–747.

PAUWELUSSEN, J. P. (1981). Nerve impulse propagation in a branching nerve system: a simple model. *Physica D* **4,** 67–88.

PAUWELUSSEN, J. (1982). One way traffic of pulses in a neuron. *J. Math. Biol.* **15,** 151–171.

ROBB-GASPERS, L. D. & THOMAS, A. P. (1995). Coordination of Ca^{2+} signaling by intercellular propagation of Ca^{2+} waves in the intact liver. *J. Biol. Chem.* **270,** 8102–8107.

ROONEY, T. A. & THOMAS, A. P. (1993). Intracellular calcium waves generated by Ins(1,4,5)P_3-dependent mechanisms. *Cell Calcium* **14,** 674–690.

SANDERSON, M. J., CHARLES, A. C., BOITANO, S. & DIRKSEN, E. R. (1994). Mechanisms and function of intercellular calcium signaling. *Mol. Cell. Endocrinology* **98,** 173–187.

SANDERSON, M. J., CHARLES, A. C. & DIRKSEN, E. R. (1990). Mechanical stimulation and intercellular communication increases intracellular Ca^{2+} in epithelial cells. *Cell Reg.* **1,** 585–596.

SNEYD, J., CHARLES, A. C. & SANDERSON, M. J. (1994). A model for the propagation of intercellular calcium waves. *Am. J. Physiol.* (*Cell Physiol.*) **266,** C293–C302.

SNEYD, J., WETTON, B., CHARLES, A. C. & SANDERSON, M. J. (1995a). Intercellular calcium waves mediated by diffusion of inositol trisphosphate: a two-dimensional model. *Am. J. Physiol.* (*Cell Physiol.*) **268,** C1537–C1545.

SNEYD, J., KEIZER, J. & SANDERSON, M. J. (1995b). Mechanisms of calcium oscillations and waves: a quantitative analysis. *FASEB J.* **9,** 1463–1472.

SNEYD, J. & SHERRATT, J. (1997). On the propagation of calcium waves in an inhomogeneous medium. *SIAM J. Appl. Math.* **57,** 73–94.

TYSON, J. J. & KEENER, J. P. (1988). Singular perturbation theory of traveling waves in excitable media. *Physica D* **32,** 327–361.

WEIDMANN, S. (1966). The diffusion of radiopotassium across intercalated disks of mammalian cardiac muscle. *J. Physiol.* **187,** 323–342.

ZYKOV, V. S. (1980). Analytic evaluation of the dependence of the speed of excitation wave in a two-dimensional excitable medium on the curvature of its front. *Biophysics* **25,** 906–911.